

35

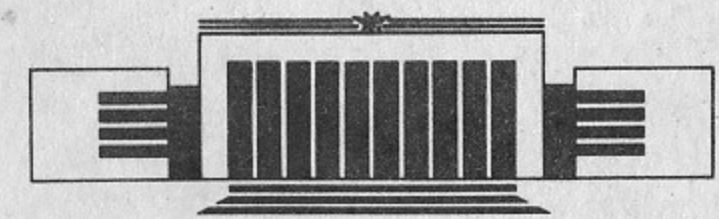
ИНСТИТУТ ЯДЕРНОЙ ФИЗИКИ СО АН СССР



Felix M. Izrailev

SCALING PROPERTIES  
OF LOCALIZED QUANTUM CHAOS

PREPRINT 91-97



НОВОСИБИРСК



# Scaling Properties of Localized Quantum Chaos<sup>\*)</sup>

Felix M. Izrailev

Institute of Nuclear Physics  
630090, Novosibirsk 90, USSR

## ABSTRACT

Statistical properties of spectra and eigenfunctions are studied for the model of quantum chaos in the presence of dynamical localization. The main attention is paid to the scaling properties of localization length and level spacing distribution in the intermediate region between Poissonian and Wigner-Dyson statistics. It is shown that main features of such localized quantum chaos are well described by the introduced ensemble of Band Random Matrices. The latter may be regarded as a generalization of the known ensemble of fully random matrices.

---

<sup>\*)</sup> A talk given on Advanced Study Workshop "Quantum Chaos-Experiment and Theory", Copenhagen (Denmark), May 1991.

## INTRODUCTION

Nowadays, much attention is paid to the properties of the so-called "quantum chaos" (see, e.g. [1-3]). The latter term is commonly used for dynamical quantum systems which are chaotic in the classical limit. Since properties of quantum systems turned out to be different from classical ones even in a deep semiclassical region (see [4-5]), one of the important problems of quantum chaos is to find proper quantities to describe the degree of chaos in quantum systems. The most known approach in this direction is related to the study of fluctuations in energy spectra in dependence of properties of correspondent classical systems. It is now well established that for systems which are integrable in the classical limit the spectrum statistics is close to uncorrelated one. Unlike, for classically completely chaotic systems the fluctuations in energy spectra are of the specific form and may be compared to that ones of eigenvalues of random matrices.

One of the quantities used to distinguish between these two limit cases is the distribution  $P(s)$  of spacings between neighbouring energy levels in the spectrum. For classically integrable systems it was conjectured [6] that  $P(s)$  is close to the Poissonian law

$$P(s) \sim \exp(-s). \quad (1)$$

Numerical experiments with some models give good evidence to this statement, also, clear deviations are known for some cases (see, e.g. discussion in [7]). In the other limit of strongly chaotic systems this distribution was found [8] to be very close to the so-called Wigner-Dyson surmise

$$P(s) = As^\beta e^{-Bs^2}, \quad (2)$$



where  $A$  and  $B$  are normalizing constants, and  $\beta$  is a parameter depending on the symmetry of the system and characterizing the repulsion between neighboring levels ( $\beta = 1, 2$ , or  $4$  for the Gaussian Orthogonal Ensemble of random matrices (GOE), Gaussian Unitary Ensemble (GUE) and Gaussian Symplectic Ensemble (GSE), respectively, see [9–10]).

Both above distributions (1) and (2) are assumed to be universal in a sense that they are not dependent on density of states which changes from one system to another. It should be stressed that spacings  $s$  are normalized to local mean value, therefore, the distribution  $P(s)$  is, in essence, some characteristic of local statistical properties of spectrum. This is in accordance to the conjecture of Wigner-Dyson approach that spectrum statistics of very complex systems is universal and can be well described by Random Matrix Theory (RMT) [9–10].

Nevertheless, it is clear that there are situations where the distribution  $P(s)$  is intermediate between Poissonian and Wigner-Dyson ones. The known example is studied in [11] where the influence of stable regions in the phase space of correspondent classical systems on the spectrum statistics has been established. The only parameter in the proposed expression for  $P(s)$  (the so-called Berry-Robnik distribution) is exactly the ratio of the area with stable motion to that of chaotic motion. There are many numerical data related to this situation (see, discussion in [2]) but the correspondence of these data to Berry-Robnik distribution turns out to be strongly dependent on the parameters of the chosen model.

To our opinion, the explanation of this fact is that the influence of quantum effects on spectrum statistics could be very strong. In this sense, it is naturally to assume that the distribution  $P(s)$  depends not on classical properties only but also on quantum ones. In the simplest case, when the model is essentially described by two parameters only, one of which is classical one,  $K$ , and another is of pure quantum nature,  $\hbar$ , the distribution  $P(s)$  seems to depend on  $K$  and  $\hbar$  both,  $P(s, K, \hbar)$ . Therefore, only in the very deep semiclassical region,  $\hbar \rightarrow 0$ , one may expect the validity of Berry-Robnik dependence.

Here, we show that there is another type of intermediate statistics which is entirely related to the quantum effects of localization. This situation appears in the case  $K \gg 1$  when in the classical limit stable regions are very small and may be neglected. The level spacing distribution  $P(s)$  in this situation seems to be universal and can be described by generalized ensemble of Band Random Matrices (BRM).

## QUANTUM CHAOS AND DYNAMICAL LOCALIZATION

### The Model of Kicked Rotator on a Torus

To study the influence of quantum effects on statistical properties of energy (or quasienergy) spectrum and eigenfunctions (EF) we consider the kicked rotator model on a torus. This model is a modification of the well known kicked rotator (KR) whose Hamiltonian has the form (see, e.g., [4–5]):

$$\hat{H} = -\frac{\hbar^2}{2I} \frac{\partial^2}{\partial \theta^2} + \varepsilon_0 \cos \theta \cdot \delta_T(t). \quad (3)$$

Here  $\delta_T(t) \equiv \sum_{m=-\infty}^{\infty} \delta(t - mT)$  is a periodic delta function with the period  $T$ , the parameter  $\varepsilon_0$  is the perturbation strength and  $I$  is the moment of inertia.

By integrating between successive kicks the motion of this model can be described by the mapping for the  $\psi$  function in one period of the perturbation:

$$\psi(\theta, t + T) = \hat{U} \psi(\theta, t) \quad (4)$$

$$\hat{U} = \exp\left(i \frac{T\hbar}{4I} \frac{\partial^2}{\partial \theta^2}\right) \exp\left(-i \frac{\varepsilon_0}{\hbar} \cos \theta\right) \exp\left(i \frac{T\hbar}{4I} \frac{\partial^2}{\partial \theta^2}\right).$$

In the above expressions the  $\psi$  function is determined in the middle of the rotations, between two successive kicks. As is seen from (4), the dynamics of our model entirely depends (apart from the initial state  $\psi(\theta, 0)$ ) on two parameters

$$\tau \equiv \frac{T\hbar}{I}; \quad k \equiv \frac{\varepsilon_0}{\hbar}. \quad (5)$$

Since without perturbation ( $k = 0$ ) the Hamiltonian (1) is time independent, the solution  $\psi(\theta, t)$  is convenient to represent in the form of an expansion in eigenfunctions of the angular momentum,

$$\psi(\theta, t) = \frac{1}{\sqrt{2\pi}} \sum_{n=-\infty}^{\infty} A_n(t) \exp(in\theta). \quad (6)$$

As a result, the mapping for the Fourier coefficients of  $\psi$  is

$$A_n(t + T) = \sum_{m=-\infty}^{\infty} U_{nm} A_m(t). \quad (7)$$



$$U_{nm} = \exp\left(i\frac{\tau n^2}{4}\right) (-i)^{n-m} J_{n-m}(k) \exp\left(i\frac{\tau m^2}{4}\right).$$

For the comparison with the classical model, it is convenient to introduce the parameter:

$$K = \tau k = \frac{T\varepsilon_0}{I}, \quad (8)$$

which does not depend on  $\hbar$ , therefore, it is a classical one. As the second independent parameter we will use  $k \sim \frac{1}{\hbar}$ , which is of a purely quantum nature. Therefore, the classical limit corresponds to  $K = \text{const.}$  with  $k \rightarrow \infty$ ,  $\tau \rightarrow 0$ .

The classical counterpart of KR is known as the "standard mapping" (see, e.g., [12-13])

$$p_{t+T} = p_t + \varepsilon_0 \sin \theta_t, \quad (9)$$

$$\theta_{t+T} = \theta_t + \frac{T}{I} p_{t+T},$$

which can be obtained from the classical Hamiltonian corresponding to (3). It can be shown that the phase space of this classical model is periodic in momentum with period  $\frac{2\pi}{T}$ .

By a rescaling of the momentum  $P \equiv \frac{T}{I} p$ , we have the standard mapping in its "standard form" where the dynamics depends, unlike the quantum model, on one parameter  $K$  only.

It is known (see [12-13] and references therein) that for sufficiently small perturbation  $K \ll 1$  in (9) the chaotic motion occurs only in small regions of phase space, in so-called stochastic layers surrounding nonlinear resonances of different harmonics. When  $K$  exceeds the critical value  $K_{cr} \simeq 1$ , the unbounded diffusion arises in momentum space for the initial conditions  $P_0, \theta_0$  outside of non-destroyed stable regions. With further increase of  $K$ , these regions are decreasing and for  $K \gtrsim 5$  they appear to be so small that for almost all initial conditions the motion turns out to be strongly chaotic. An essential property of chaotic motion, in view of comparison with the behavior of the quantum model (3), is the diffusive growth of momentum,  $\langle (P - P_0)^2 \rangle = D_{cl} t$ . Here,  $D_{cl} \approx \frac{K^2}{2}$  is the classical diffusion coefficient, and the averaging is performed over the set of trajectories initially located in a small region of phase space.

The numerical experiments [4-5] have shown that, in contrast with the classical model, for a large value of the classical parameter  $K = 5$  and a large parameter  $k \gg 1$ , therefore, in a deep semiclassical region, the correspondence of the quantum behavior to the classical diffusion holds only for some characteristic time  $t \gtrsim t^*$ . After this time, for  $t \lesssim t^*$  the growth of the rotator energy is decreasing in time, and for sufficiently large time the diffusion appears to be completely suppressed. This phenomenon, termed in [5] "quantum suppression" of the classical chaos, was found to be a generic property and results in weak statistical properties both of quasienergy spectra and eigenfunctions [7].

Unlike the above model with infinite number of states (the momentum space is unbounded), we pass to the model with finite number of states. It allows to follow the whole transition from weak to strong statistical properties of quantum chaos. This model can be deduced from (3) (see details in [7]) and corresponds, in the classical limit, to the standard mapping on a torus of size  $\frac{2\pi m_0}{T}$  in the momentum  $p$ . The quantization conditions are  $N = \frac{2\pi m_0}{T\hbar}$  and  $\tau = \frac{4\pi r}{N}$  where  $N$  is the total number of states ( $N\tau = \text{const}$  when  $N \rightarrow \infty$ ) and  $m_0$  is an integer.

As a result, the evolution unitary matrix  $U_{nm}$  is finite of size  $N$  and has the form [7]

$$U_{nm} = e^{i\frac{\tau}{4}n^2} \frac{1}{N} \sum_{l=-N_1}^{N_1} e^{-ik \cos(\frac{2\pi}{N}l)} e^{-i\frac{2\pi}{N}l(n-m)} e^{i\frac{\tau}{4}m^2}, \quad (10)$$

where  $n, m = -N_1, \dots, N_1$  and  $N = 2N_1 + 1$ .

Our main interest is in the study of statistical properties of the quasienergy spectrum  $\varepsilon$  and eigenfunctions  $\varphi_n(\varepsilon)$  which are defined by the equation

$$e^{-i\varepsilon} \varphi_n(\varepsilon) = \sum_m U_{nm}(k, \tau) \varphi_m(\varepsilon), \quad (11)$$

where  $U_{nm}$  is given by (10).

### Maximal Statistical Properties of Quantum Chaos

In the limit case of small perturbation,  $k \ll 1$ , the level spacing distribution  $P(s)$  was found [7] to be very close to the Poissonian distribution (2). In other limit case of very strong perturbation,  $k \rightarrow \infty$ , we may expect that the distribution  $P(s)$  approaches the Wigner-Dyson distribution (2). However, as it was shown in [14] (see also [15]), the physical parameter which determines



the validity of the expression (2) is not the strength parameter  $k$  but the ratio of the localization length  $l_\infty$  to the total number of states  $N$

$$\Lambda = \frac{l_\infty}{N}. \quad (12)$$

Here, the average localization length  $l_\infty$  characterizes the exponential localization of eigenvectors  $\varphi_n(\varepsilon)$  of the evolution operator (7) in the unbounded momentum space,  $\varphi_n \sim \exp(-|n - n_0|/l_\infty)$  for  $|n| \rightarrow \infty$  (see e.g. [7]).

One of the most important results of numerical simulations is the remarkable relation between the average localization length  $l_\infty$  and the classical diffusion coefficient  $D_{cl}$ :

$$l_\infty \simeq \frac{D_{cl}(K)}{2\tau^2} \simeq \frac{k^2}{4}. \quad (13)$$

Here, the relation  $D_{cl} \simeq \frac{K^2}{2}$  is used which is valid for large  $K \gg 1$  (also, for  $K \approx 5$ , see [12–13]) and  $l_\infty$  is given in number of unperturbed levels.

Extensive numerical data have shown [14,16–17] that under the condition of strong classical chaos,  $K \gg 1$ , and for delocalization of all eigenfunctions (EF),  $\Lambda \gg 1$ , statistical properties of quasienergy spectrum and EFs are well described by Random Matrix Theory [9–10]. In particular, the level spacing distribution  $P(s)$  is very close to the Wigner–Dyson dependence (2). Also, the distribution of components  $\varphi_n$  of EF in the unperturbed basis for large  $N \gg 1$  is very close to Gaussian distribution

$$W_N(\varphi_n) = \sqrt{\frac{N}{2\pi}} e^{-\frac{N}{2}\varphi_n^2}. \quad (14)$$

It is important to emphasize that our unitary matrix (10) is not random by construction and depends on two dynamical parameters,  $\tau$  and  $k$ , only. Nevertheless, under two conditions (strong classical chaos and delocalization of quantum states) the maximal statistical properties of quantum chaos are similar to that known for eigenvalues and eigenvectors of random matrices.

### Intermediate Statistics for Level Spacing Distribution

To illustrate the influence of quantum effects on the quasienergy statistics, we present here the data for  $P(s)$  when classical parameter  $K$  is fixed,  $K = 5$  but quantum parameter  $k$  ranges in such a way that  $\Lambda$  goes to zero. In Fig.1 typical examples of  $P(s)$  are given for three values of  $k$ . Here  $s$  stands for the normalized spacings  $s_j = \frac{N}{2\pi}(\varepsilon_{j+1} - \varepsilon_j)$  which are found from the eigenvalues

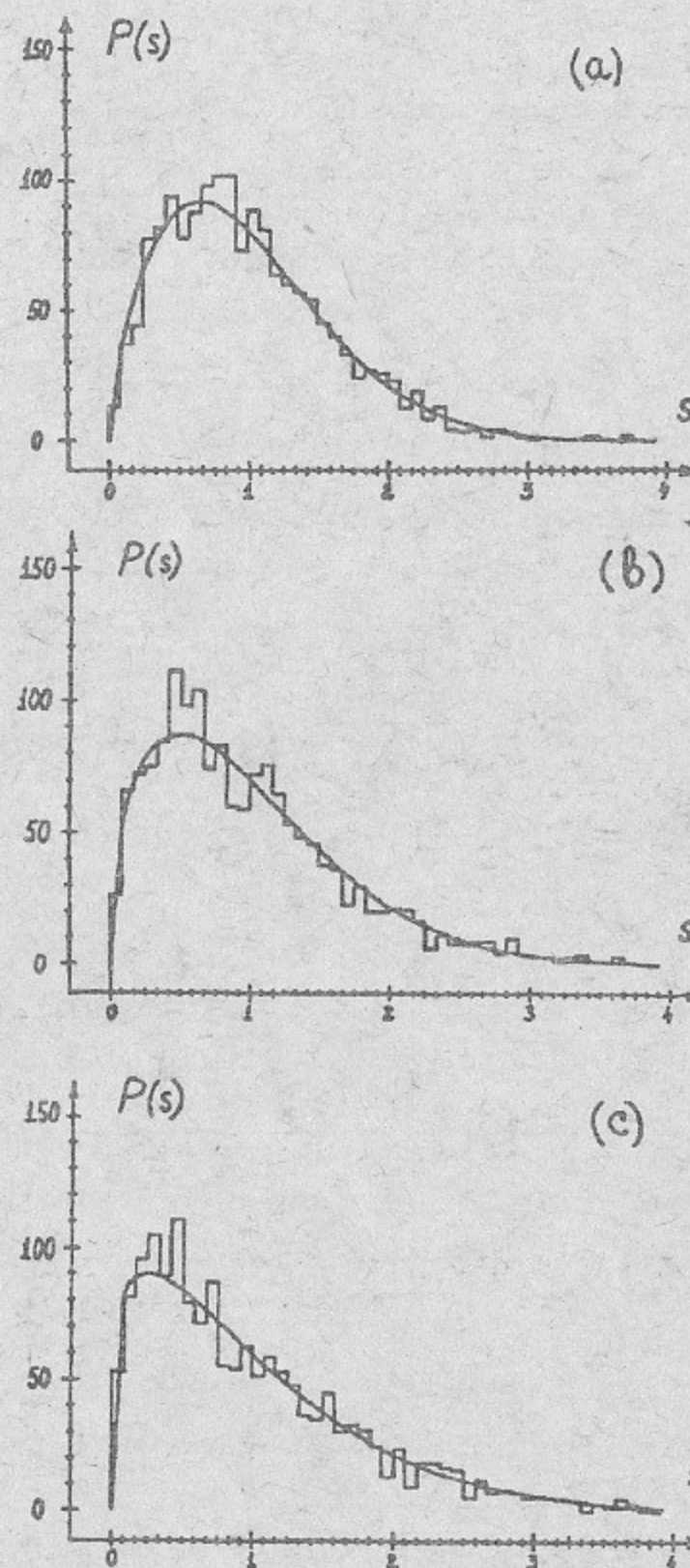


Fig. 1. Three examples of the intermediate statistics for  $P(s)$  for the model (10) with  $N = 398$  and  $K = 5$ . The total number of quasienergy levels is  $M = 1592$ . The staggered curve is the numerical data. The smooth curve is the dependence (15). a)  $k \approx 39.8; \beta \approx 0.76; \Lambda \approx 1.0$ ; b)  $k \approx 21.1; \beta \approx 0.48; \Lambda \approx 0.3$ ; c)  $k \approx 9.1; \beta \approx 0.22; \Lambda \approx 0.05$ ;



$\lambda_j = \exp(i\varepsilon_j)$  of the unitary matrix (10). To improve the statistics, the distributions  $P(s)$  for four matrices (10) of size  $N = 398$  have been summed with slightly different values of  $k$  ( $\delta k \ll k$ ). The total number of spacings in each histogram is  $M = 1592$ . It is clearly seen that with the decrease of  $\Lambda$  the distribution  $P(s)$  approaches the Poissonian law.

The full lines in Fig.1 correspond to the distribution

$$P(s) = As^\beta \exp \left[ -\frac{\pi^2}{16} \beta s^2 - \frac{\pi}{2} \left( B - \frac{\beta}{2} \right) s \right], \quad (15)$$

which has been introduced in [18] to describe the intermediate statistics for  $P(s)$ . Here, the parameters  $A$  and  $B$  are determined by the normalization conditions

$$\int_0^\infty P(s) ds = 1; \quad \int_0^\infty sP(s) ds = 1. \quad (16)$$

The expression (15) has the only unknown parameter  $\beta$  which can be non-integer, unlike the Wigner-Dyson distribution (2). Peculiarity of the dependence (15) is that it appears to be quite close to the Wigner-Dyson dependence (2) for  $\beta = 1; 2; 4$  in (2) (see [7,18]). In addition, for  $\beta = 0$  it is exactly a Poissonian distribution. Therefore, this expression can be used to approximately describe the whole transition from uncorrelated (Poissonian) statistics to the limiting Wigner-Dyson statistics (2) with the specific value of  $\beta$  which is defined by the symmetry of the system. The values of  $\beta$  for the data of Fig.1 are taken to correspond to the mean localization length  $l_N$  of eigenfunctions defined in [18] for the systems with finite number of states (see below). Good numerical agreement between the numerical data and the expression (15) is clearly seen, which is also supported by the  $\chi^2$  approach. Specifically, for  $\Lambda \approx 1.0, 0.3$  and  $0.05$  ( $\beta \approx 0.76, 0.48$  and  $0.22$ , respectively), the  $\chi^2$  values for 23 subintervals are  $\chi_{23}^2 \approx 15.6, 27.2$  and  $28.5$ , which gives for the confidence levels 90%, 30% and 35%, respectively.

### Localized chaotic states

As it was shown in [18], the intermediate statistics is closely related to the structure of eigenstates. In particular, with the decrease of the quantum parameter  $k$  "the effective size" of eigenstates in the momentum space decreases. It is illustrated in Fig.2 where typical form of EFs is given for two values of  $\Lambda$ . The important peculiarity is that on some scale, all eigenstates seem to have

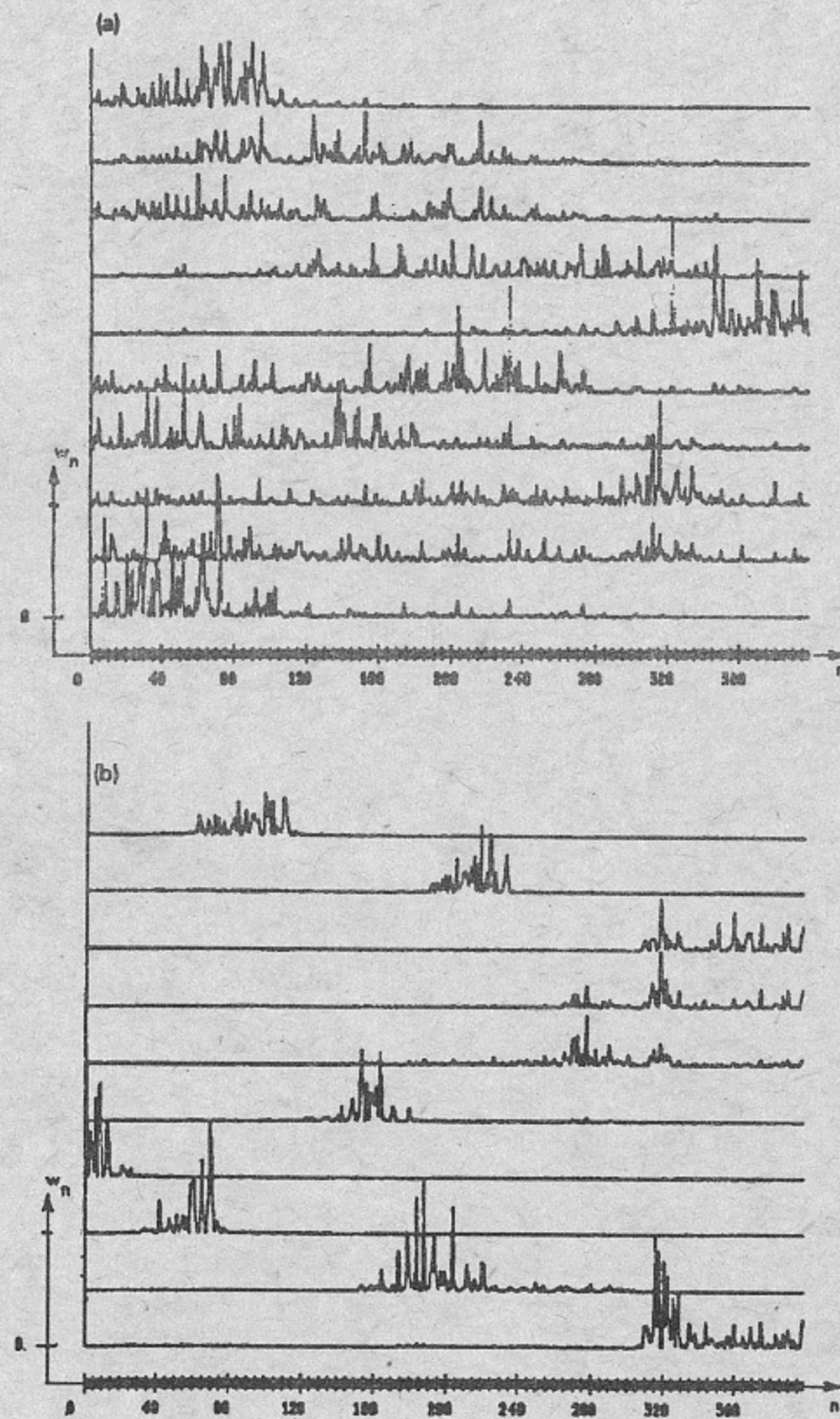


Fig. 2. Ten out of  $N = 398$  eigenstates of the model (15) are shown. On the vertical axis the probability  $w_n = |\varphi_n|^2$ ; on the horizontal axis the number of unperturbed state,  $n$ . The parameters are (a)  $K \approx 5, k \approx 32.0, \tau \approx 0.158, \Lambda \approx 0.64$ ; (b)  $K \approx 5, k \approx 10.6, \tau \approx 0.47, \Lambda \approx 0.07$ .



chaotic structure. To measure this scale, in [18] new definition of localization length has been introduced (see also [7] and references therein):

$$l_N = N \exp(\langle H \rangle - H_R), \quad (17)$$

which is based on computing the spectral entropy of eigenstates:

$$H = - \sum_{n=1}^N w_n \ln w_n; \quad w_n = |\varphi_n|^2. \quad (18)$$

The averaging of (18) in (17) is performed over all eigenstates of one matrix  $U_{nm}$  or over an ensemble of matrices with slightly different values of  $\Lambda$ . The normalizing coefficient  $H_R$  in (17) is, in essence, the limiting entropy which corresponds to the completely chaotic eigenstates (see (14)). In this definition the averaged localization length  $l_N$  scales from 1 to  $N$  with the increase of  $\Lambda$ . This definition is closely related to the simple approach that measures localization length as an effective size on which the main probability of EF is concentrated.

### Scaling Properties of Eigenfunctions and Spectrum Statistics

The main idea of our approach is that the intermediate statistics due to localization has universal scaling properties. More exactly, in [19] was numerically proved that in large range of values  $\Lambda$  the level spacing distribution depends on the scaling parameter  $\Lambda$  only, rather than on two parameters  $k$  and  $N$  separately. It means that for the same value  $\Lambda$  but different values of  $k$  and  $N$  in the model (10) the distribution  $P(s)$  is the same. Numerical evidence for this statement is presented in Fig.3 where two distributions  $P(s)$  are compared with fixed value  $\Lambda \approx 0.8$  and different  $k, N$ . The fit to the dependence (15) by the  $\chi^2$  approach has been used to obtain the effective repulsion  $\beta$ . The dashed lines are 1% deviations (for the  $\chi^2$  value) from the best fit. A few matrices (10) were used to improve statistics, with slightly different values of  $k$ . The numerical data show that the fit repulsion parameter  $\beta$  in the expression (15) is approximately the same.

The localization length  $l_N$  introduced by (17) may be associated with the localization length  $\xi_N$  in solid state models for finite samples of size  $N$ . Then, according to the approach developed in [20], some scaling for  $l_N$  can be also expected. Indeed, the localization in solid state physics in finite samples is related to the residual conductance of the samples themselves. The corner of the scaling theory of localization is the assumption that conductance depends

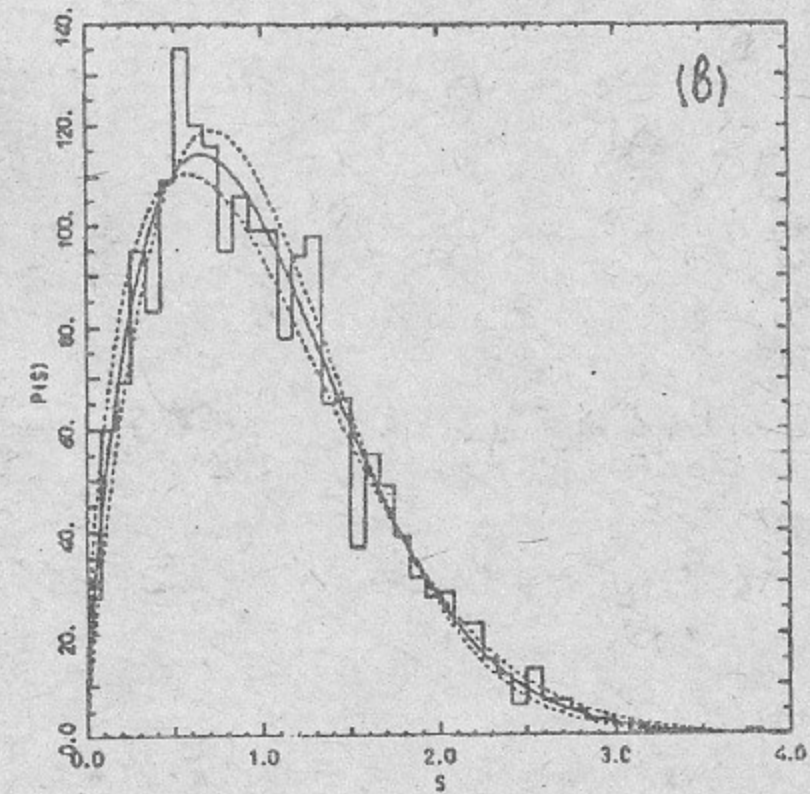
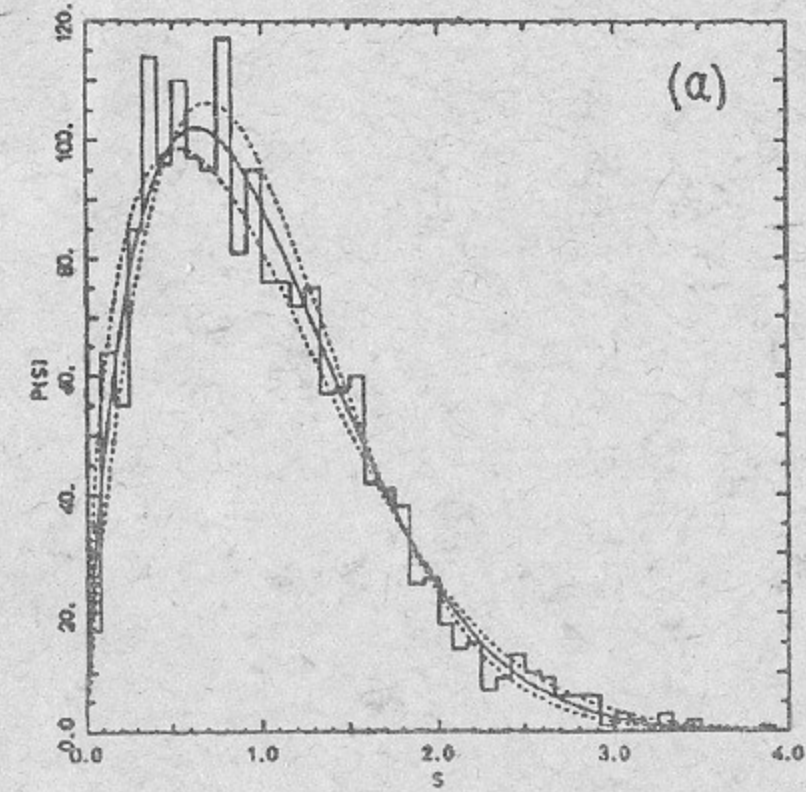


Fig. 3. The scaling distribution  $P(s)$  for the model (10) with different sizes  $N$  of the basis for  $K = 5$  and  $k^2/N \approx 2.5$ . The solid lines correspond to the best fit to relation (15) by the  $\chi^2$  approach. The value of rescaled period  $\tau$  is  $\tau = 4\pi r/(2N + 1)$ . (a)  $N = 600, k \approx 35.0, r = 14, \beta \approx 0.67, \beta_{min} \approx 0.50, \beta_{max} \approx 0.83$ ; (b)  $N = 200, k \approx 22.8, r = 7, \beta \approx 0.70, \beta_{min} \approx 0.55, \beta_{max} \approx 0.86$ .



only on the ratio between the localization length for the infinite sample and the size of the sample. This conjecture can be formulated (see details in [20]) in the way that there is a universal function  $g(z)$  such that

$$\frac{\xi_N}{\xi_\infty} = g(z); \quad z = \frac{N}{\xi_\infty} \quad (19)$$

where  $\xi_\infty$  has the same meaning as (13), namely, the localization length for an infinite sample. In the approach of Ref. [20] the quantity  $\xi_N$  is directly related to the residual conductance via Landauer's formula and can be defined by means of the transfer-matrix formalism. Therefore, the scaling

$$\beta^* = \frac{l_N}{N} = f\left(\frac{\tilde{D}}{N}\right); \quad \tilde{D} = \frac{D_{cl}}{\tau^2} \quad (20)$$

is expected to exist for the KR-model (10) where  $D_{cl}$  stands in place of  $l_\infty$ . Numerical simulation with the model (10) has been performed to check this conjecture (see details in [19]). For this, the quantity  $l_N$  has been computed through (17-18) for many different values of  $N$  and  $k$  in the ranges  $200 \leq N \leq 860$  and  $1 < k \leq 239$ . The classical parameter was taken in all cases as  $K \approx 5$ , therefore,  $\tilde{D} \approx \frac{k^2}{2}$ . The data are shown in Fig.4 which gives a good evidence of scaling in the mean. The insert in Fig.4 is also shown to follow the linear dependence  $\beta^* \sim \frac{k^2}{N}$  which has to hold for  $1 \ll l_\infty \ll N$ . It is seen that the latter condition is quite a strong restriction for the numerical simulation in this region and it causes the deviation of  $\beta^*$  from the straight line.

It is now clear that there is relation between the repulsion parameter  $\beta$  in (15) and the normalized localization length  $\beta^*$ . The analytical form of this relation is still not established but, according to the data [19], for the model (10) of kicked rotator on a torus it is close to linear one,  $\beta \approx \beta^*$ .

## STATISTICAL PROPERTIES OF BAND RANDOM MATRICES

### Definition of the Ensemble of Band Random Matrices

The unitary matrix  $U_{nm}$  for the KR-model on the torus appears to have a band structure with the size of the band ( $\approx 2k$ ) determined by the quantum parameter  $k$  (see (10)). At the same time, the classical parameter  $K$  seems to be responsible for the degree of randomness of matrix elements inside this band. It leads to the conjecture that statistical properties of the KR-model

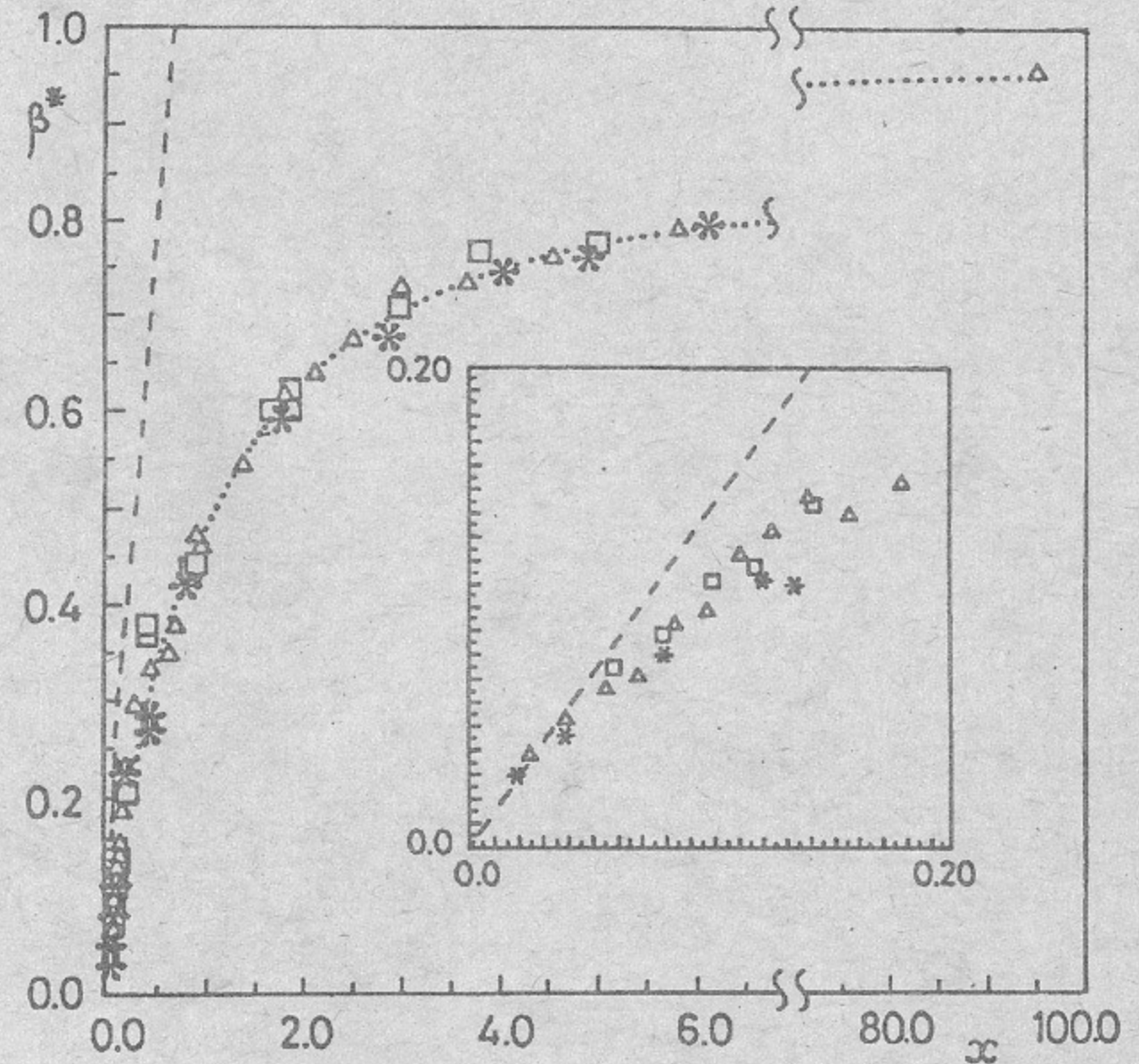


Fig. 4. The parameter  $\beta^*$  versus the variable  $x = k^2/N$  for  $N \approx 400$  ( $\square$ ),  $N \approx 600$  ( $\triangle$ ) and  $N \approx 800$  ( $*$ ) is plotted for the model (10). The dashed lines correspond to the expression  $d \approx 2el_\infty$  which is expected for  $x \ll 1$  (see [7]). The dotted curve gives the fit in the intermediate region when passing from localized to delocalized states.



(10) for large  $K \gg 1$  are also typical for the ensemble of Band Random Matrices.

The structure of such real symmetric matrices is given by the parameter  $b$  determining the band size,  $b$  equals 1 for diagonal, 2 for tridiagonal and  $N$  for GOE matrices. Inside the band, for  $|i - j| < b$ , matrix elements  $a_{ij}$  are independent gaussian numbers with the mean equal to zero and the variance corresponding to the probability density

$$\begin{aligned} P(A_{ii}) &= \sqrt{\omega/\pi} \exp(-\omega A_{ii}^2), \\ P(A_{ij}) &= \sqrt{2\omega/\pi} \exp(-2\omega A_{ij}^2) \quad i < j \end{aligned} \quad (21)$$

while outside the band all matrix elements equal zero.

The ensemble is fully characterized by the three parameters  $\omega$ ,  $b$  and  $N$ ; however, the first parameter only determines the size of the eigenvalues and is not relevant for describing statistical properties. As it was shown numerically in [21] and proved analytically in [22], the eigenvalue density  $\rho(\lambda)$  of BRM in the limit case of large  $N \rightarrow \infty$  has the semicircle form

$$\rho(\lambda) = \frac{2}{\pi r^2} \sqrt{r^2 - \lambda^2}. \quad (22)$$

It has second moment  $\langle \lambda^2 \rangle = r^2/4$  where  $r^2 = 2F/(N\omega)$  and  $F = \frac{1}{2}b(2N - b + 1)$  is the number of independent nonzero matrix elements.

One should note that such band matrices seem to be very convenient in describing the statistical properties of different physical systems, for example, complex atoms and nuclei (see [23-24]).

#### Scaling Properties of Eigenvectors of BRM

Numerical simulation [21] has given good evidence that the structure of EF is very similar to that found for the KR on the torus. In particular, for  $\tilde{x}$  sufficiently large ( $\tilde{x} \gtrsim 10$ ), all eigenfunctions have chaotic structure with the distribution of components very close to (14). But the most important is that in the intermediate situation, for not large  $\Lambda$  structure of eigenvectors is also very similar to that found for the kicked rotator model (10) on a torus when  $K \gg 1$  (see Fig.2).

As for the kicked rotator, numerical experiments have proved the similar scaling for the localization length  $l_N$  (see details in [7]). One of the essential results of this study is represented in Fig.5 where the dependence of  $\beta^*$  is plotted versus the scaling parameter  $b^2/N$  for different values of  $N$  and  $b$ . The smooth curve is here the function

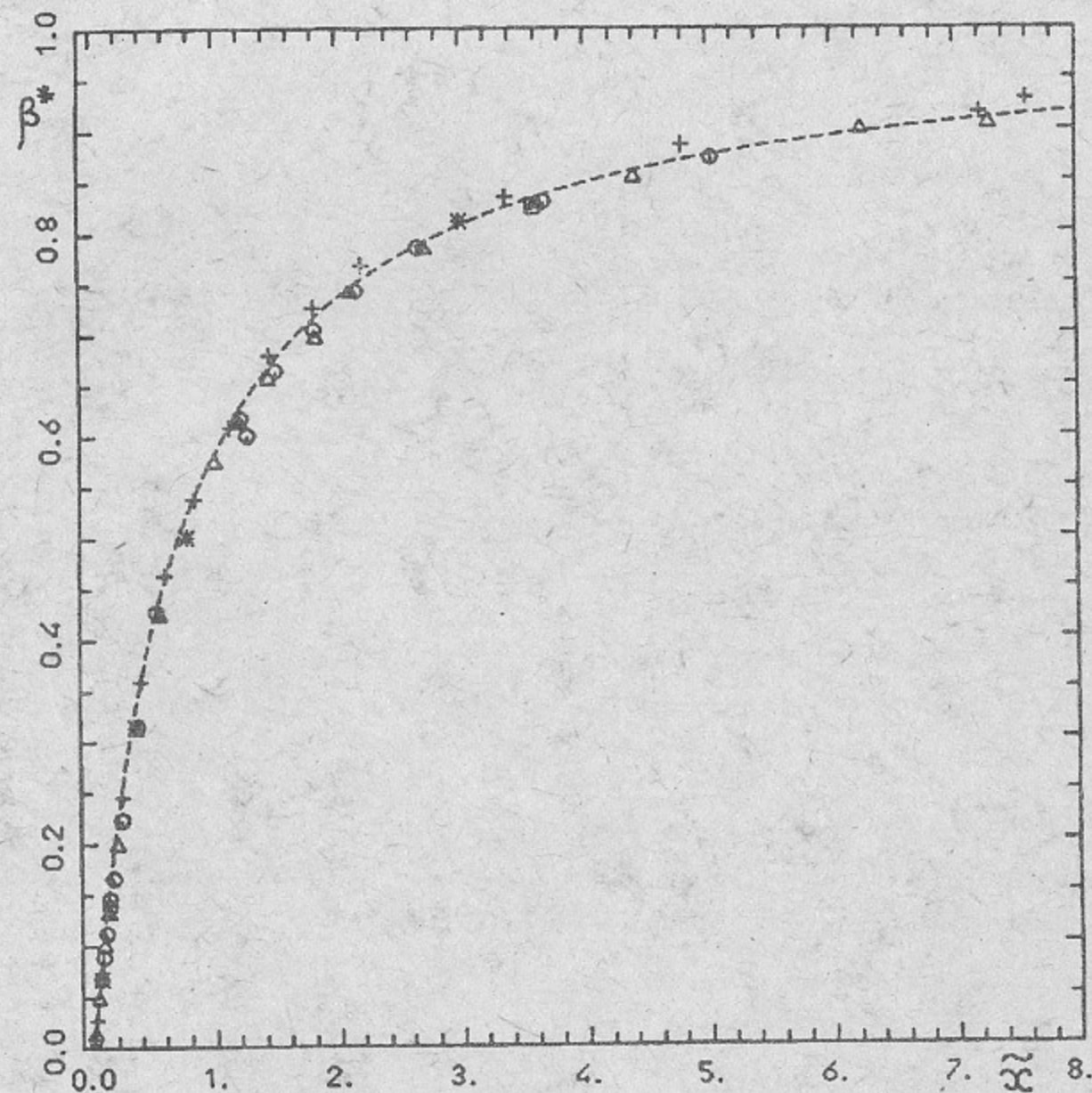


Fig. 5. The scaled localization length  $\beta^* = l_N/N$  versus  $\tilde{x} = b^2/N$  for  $N = 200$  (+),  $N = 400$  ( $\Delta$ ),  $N = 600$  ( $\circ$ ),  $N = 800$  ( $\star$ ) and  $N = 1000$  ( $\square$ ). The dashed curve corresponds to the expression (23).



$$\beta^* = \frac{C\tilde{x}}{1 + C\tilde{x}}, \quad (23)$$

where the parameter  $C$  is taken to be  $C \approx 1.4$  from the data for the KR-model (see Fig.3) with the correspondence of  $b$  to  $k$ . It is seen that the scaling behavior

$$\frac{l_N}{N} = f(\tilde{x}); \quad \tilde{x} = \frac{b^2}{N} \quad (24)$$

is very impressive. However, one should note that, unlike the parameter  $k$  in the KR-model, the parameter  $b$  in BRM is restricted by the maximal value  $N$ . For this reason the scaling  $\beta^*(\tilde{x})$  holds only for  $b \lesssim N/2$ . For  $b \rightarrow N$ , the similarity with KR disappears and another behavior of  $\beta^*$  occurs [21].

### Scaling Properties of Level Spacing Distribution

In analogy with kicked roator model (10) it is natural to expect that the distribution  $P(s)$  of spacings between neighbouring eigenvalues of BRM is essentially dependent on the parameter  $\tilde{x}$  only, rather than on  $b$  and  $N$  independently. As it is known, in the extreme case of diagonal matrices ( $b = 1$ ) the spacings between eigenvalues are not correlated, resulting in the Poisson distribution for  $P(s)$ . On the other hand, in the opposite case of fully random matrices ( $b = N$ ), the RMT predicts the Wigner-Dyson form (2).

To describe the intermediate statistics  $P(s)$  for BRM where  $P(s)$  changes from Poisson to Wigner-Dyson distribution, in [25] the improved version of the phenomenological dependence (15) has been used

$$P(s) = As^\beta (1 + B\beta s)^{f(\beta)} \exp \left[ -\frac{\pi^2}{16} \beta s^2 - \frac{\pi}{2} \left(1 - \frac{\beta}{2}\right) s \right], \quad (25)$$

where  $A$  and  $B$  are normalizing parameters and

$$f(\beta) = \frac{2^\beta (1 - \frac{\beta}{2})}{\beta} - 0.16874 \quad (26)$$

is some characteristic function.

For  $\beta = 0$  the expression (25) reduces to the Poisson distribution and for  $\beta = 1, 2, 4$  it approximates very closely the  $P(s)$  distribution for Gaussian orthogonal, unitary and symplectic ensembles (GOE, GUE, GSE). Expression (25) is more complicated than (15), but it gives a much better correspondence

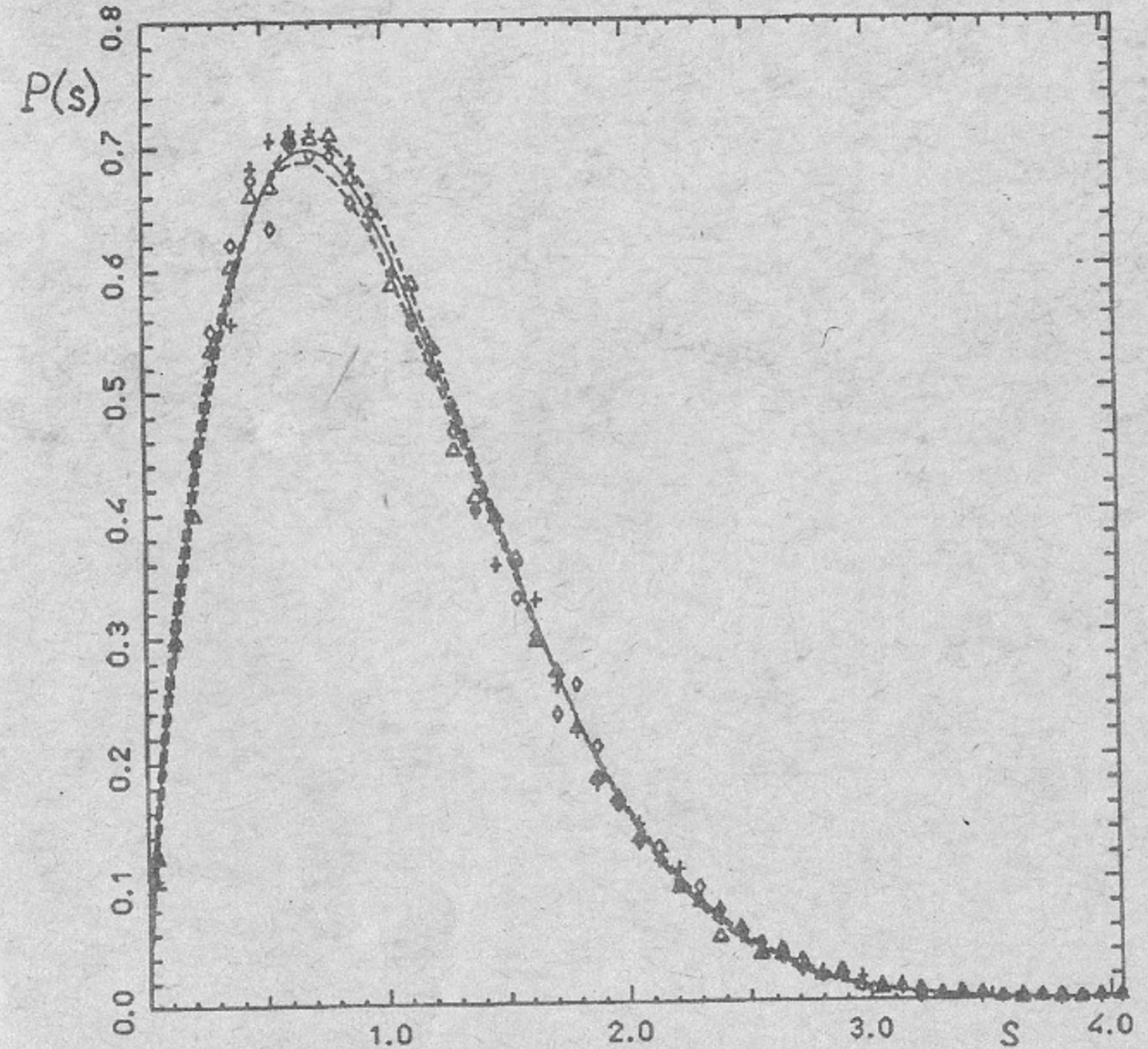


Fig. 6. The level spacing distribution  $P(s)$  for  $\tilde{x} = b^2/N \approx 1$  with  $N = 400$  (+),  $N = 800$  ( $\Delta$ ),  $N = 1600$  ( $\diamond$ ). The full curve corresponds to the expression (25) with the best fitting value  $\beta = 0.703$  found for  $N = 800$ . The dashed curves give the lower and upper bounds for 1% confidence level with  $\beta_- = 0.620$  and  $\beta_+ = 0.759$  respectively.



with RMT predictions. For example, for  $\beta = 1$  the deviation from the exact dependence of  $P(s)$  is less than 0.3 % for small ( $s \leq 0.1$ ) and large ( $s \geq 2$ ) spacings; it is less than 0.02 % in the most important intermediate region  $0.5 \leq s \leq 1.6$ . This distribution is thus closer to the exact one than Wigner's distribution (2) itself. The agreement with RMT is very good also for  $\beta = 2, 4$ . In addition, the dependence (25) seems to be more suitable to fit the numerical data for the intermediate statistics  $P(s)$  than the commonly used Brody distribution [26] (see discussion in [7,18]).

In numerical experiments [25] BRM-matrices have been used with sizes  $N = 400, 800, 1600$  and different band sizes  $b \gg 1$ . The distribution  $P(s)$  was obtained by averaging over the  $P(s)$  for  $Q$  different random matrices with the same  $N$  and  $b$  ( $Q = 50, 25, 12$  for  $N = 400, 800, 1600$ , respectively). Since the eigenvalue density is not uniform, the spacings have been normalized to the local density. To avoid the influence of large fluctuations caused by the finite size of matrices, a number of eigenvalues at the edges of the semicircle distribution (22) has not been taken into account. As a result, for each  $N$  and  $b$ , the total number of spacings in the final distribution of  $P(s)$  is approximately equal to  $M = 16000 - 17000$ .

A few examples of  $P(s)$  with the best fit (full curve) of the proposed dependence (25) are presented in Fig.6. Here, the parameter  $\tilde{x}$  is taken to be approximately constant,  $\tilde{x} \approx 1.0$ , while the band size  $b$  and the size  $N$  of the matrices vary. The data give good evidence for the scaling behaviour of the spacing distribution  $P(s)$ . To show the accuracy of the fit, two curves are also drawn, corresponding to the the 1%-confidence level.

The summarized data for different values of  $\tilde{x}$  are given in Fig.7. It is seen that the scaling behaviour for the repulsion parameter  $\beta$  occurs in a large range of the parameter  $\tilde{x}$ . This result indicates that fluctuations in the eigenvalue spectra of BRM appear to have universal properties which can be described by a single parameter  $\tilde{x}$ .

## CONCLUSIONS

All these results show a very deep similarity of the statistical properties of localized quantum chaos in dynamical models to that existing in random models, like the BRM ensemble. The most important result is that both properties of localized chaotic eigenstates and level spacing distribution  $P(s)$  have very similar scaling.

Scaling properties similar to those described here should be expected in

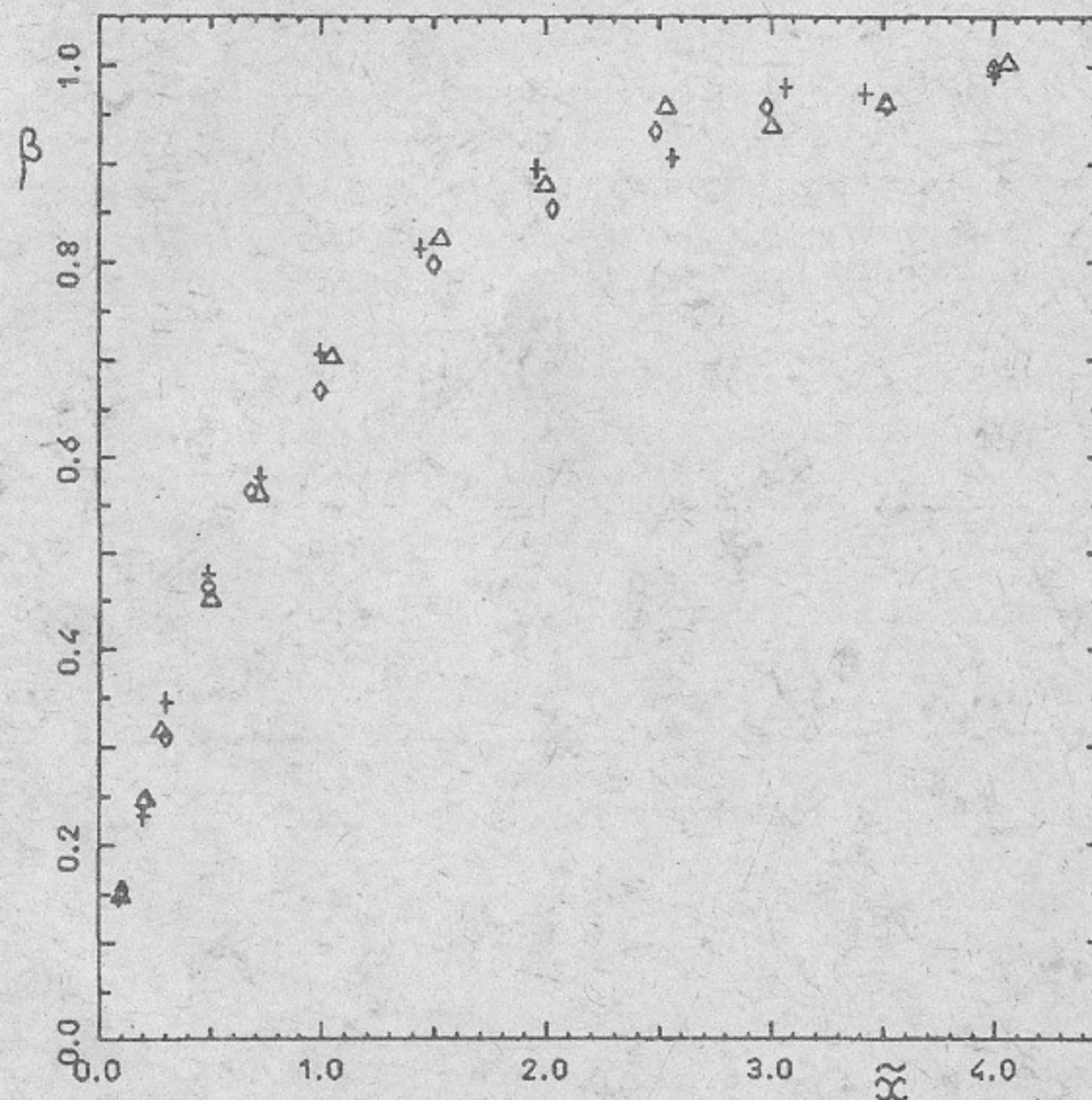


Fig. 7. The repulsion parameter  $\beta$  for intermediate statistics  $P(s)$  versus  $\tilde{x} = b^2/N$ , for different values of  $N$  and  $b$ .  $N = 400$  (+),  $N = 800$ ( $\Delta$ ) and  $N = 1600$ ( $\diamond$ ). Each value of  $\beta$  was obtained by fitting the numerical data for level spacing distribution with the expression (25). All values of  $\beta$  are within a 1% confidence level.



more realistic situations where the sharp band structure is replaced by a sufficiently fast decay of matrix elements away from the diagonal. A support to the above conclusion can be found in [22,27,28].

According to Wigner-Dyson approach, the fluctuations of spectra of full random matrices have universal properties in the sense that they appear in different complex quantum systems in spite of different density of states. Nevertheless, it is clear that full random matrices can be used to describe only limiting situation of maximal statistical properties. At the same time, most physical systems seem to relate to matrices with a band structure reflecting the finite range of interaction between unperturbed states. The results presented here lead us to the conjecture that in the intermediate case of localized quantum chaos with level spacing distribution between Poisson and Wigner-Dyson, fluctuation properties may also have universal character. For example, as it was shown, the kicked rotator model on a torus and BRM have similar fluctuation properties both for spectra and eigenfunctions, in spite of the fact that the density of states is completely different (semicircle for BRM and uniform distribution of quasienergies for kicked rotator).

#### REFERENCES

1. B.Eckardt, *Phys. Rep.* 163, 205 (1988).
2. P.V.Elyutin, *Usp. Fiz. Nauk* 155, 397 (1988).
3. Proc. Les Houches Summer School on Chaos and Quantum Physics, Elsevier, 1990.
4. G.Casati, B.V.Chirikov, J.Ford and F.M.Izrailev, *Lect. Notes Phys.* 93, 334 (1979).
5. B.V.Chirikov, F.M.Izrailev and D.L.Shepelyansky, *Sov. Sci. Rev. C* 2, 209 (1981).
6. M.V.Berry, *J. Phys. A* 10, 2083 (1977).
7. F.M.Izrailev *Phys. Rep.* 196, 299 (1990).
8. O.Bohigas and M.-J. Giannoni, *Lect. Notes Phys.* 209, 1 (1984).
9. M.L.Mehta, *Random Matrices (Academic Press, New York)* 1967.
10. T.A.Brody, J.Flores, J.B.French, P.A.Mello, A.Pandey and S.S.M.Wong, *Rev. Mod. Phys.* 53, 385 (1981).

11. M.V.Berry and M.Robnik, *J. Phys. A* 17, 2413 (1984).
12. B.V.Chirikov, *Phys. Rep.* 52, 263 (1979).
13. A.L.Lichtenberg and M.A.Liberman, *Regular and Stochastic Motion (Springer, Berlin)* 1983.
14. B.V.Chirikov, F.M.Izrailev, and D.L.Shepelyansky, *Physica D* 33, 77 (1988).
15. T.Dittrich and U.Smilansky, *Nonlinearity* 4/1, 59 (1991).
16. F.M.Izrailev, *Phys. Rev. Lett.* 56, 541 (1986).
17. F.M.Izrailev, *Phys. Lett. A* 125, 250 (1987).
18. F.M.Izrailev, *Phys. Lett. A* 134, 13 (1988); *J. Phys. A* 22, 865 (1989).
19. G.Casati, I.Guarneri, F.Izrailev and R.Scharf, *Phys. Rev. Lett.* 64, 5 (1990).
20. J.L.Pichard, *J. Phys. C* 19, 1519 (1986).
21. G.Casati, L.Molinari, and F.Izrailev, *Phys. Rev. Lett.* 64, 16 (1990).
22. Y.V.Fyodorov and A.D.Mirlin, *Scaling Properties of Localization in Random Band Matrices: A  $\sigma$ -vodel Approach*, *Phys. Rev. Lett.*, (1991) to appear.
23. B.V.Chirikov, *Phys. Lett. A* 108, 68 (1985).
24. M.Feingold, D.M.Leitner and O.Piro, *Phys. Rev. A* 39, 6507 (1989).
25. G.Casati, F.M.Izrailev and L.Molinari, *Scaling Properties of Eigenvalue Spacing Distribution for Band Random Matrices*, (1991) to be published.
26. T.A.Brody, *Lett. Nuovo Cimento* 7, 482 (1973).
27. T.H.Seligman, J.J.M.Verbaarschot and M.R.Zirnbauer, *Phys. Rev. Lett.* 53, 215 (1985).
28. T.Cheon, *Phys. Rev. Lett.* 65, 529 (1990).



*F. Izrailev*

**Scaling Properties of Localized Quantum Chaos**

*Ф. Израйлев*

**Скейлинговые свойства локализованного  
квантового хаоса**

Ответственный за выпуск С.Г. Попов

---

Работа поступила 1 октября 1991 г.

Подписано в печать 2.10 1991 г.

Формат бумаги 60×90 1/16 Объем 1,3 печ.л., 1,0 уч.-изд.л.

Тираж 290 экз. Бесплатно. Заказ N 97

---

Ротапринт ИЯФ СО АН СССР,

*Новосибирск, 630090, пр. академика Лаврентьева, 11.*